

# Hydrogen evolution reaction using EC-MS system

## EC-MS Application Note #3

last updated 06-10-2022

### Introduction

#### The hydrogen evolution reaction

The hydrogen evolution reaction (HER) is paramount for many renewable energy storage and conversion schemes, proposed for a sustainable energy economy [1]. For a simplified overview of such an energy scheme incorporating polymer electrolyte membrane electrolyzers (PEMEs) and polymer electrolyte membrane fuel cells (PEMFCs), see figure 1.

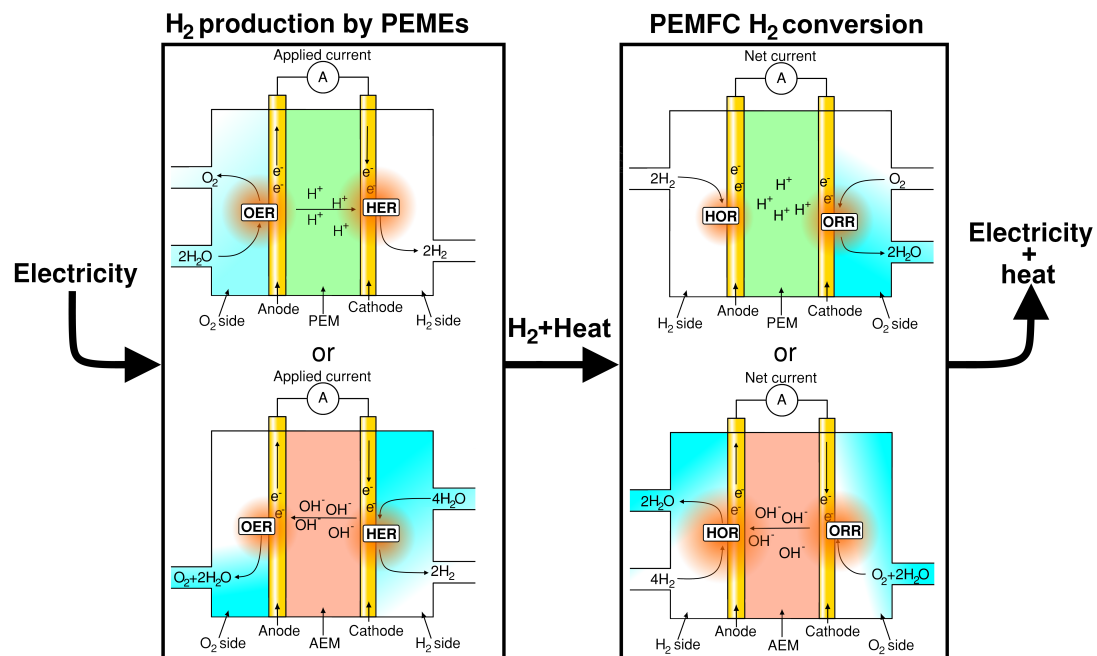


**Figure 1:** H<sub>2</sub> energy scheme: Renewable electricity powers the H<sub>2</sub> electrolyzers, produced H<sub>2</sub> can then be used in industry, as a fuel or stored to later generate electricity using a fuel cell. This scheme presents H<sub>2</sub> as an energy carrier for renewably generated electric power.

While Pt is an excellent, although scarce and expensive, catalyst material for HER in acid (for proton exchange membranes (PEMs)), significant overpotentials are experienced in alkaline electrolyzers [2–4], *e.g.* for anion exchange membranes (AEMs). Hence, research is presently being undertaken for finding:

1. Active and stable HER catalysts capable of operating under alkaline conditions.
2. Active and stable non-platinum-based metal (non-PGM) HER catalysts capable of operating in acidic conditions.

Moreover, *in lieu* of the rate determining steps of HER, finding good catalyst candidates for HER will subsequently also produce good candidates for facilitating the hydrogen oxidation reaction (HOR) for hydrogen driven PEM and AEM fuel cell applications [5].

## The importance of parasitic processes

When measuring HER catalyst activity, it is important to consider that especially in potentiodynamic measurements, the measured electrochemical currents do not always solely derive from H<sub>2</sub> evolution. Rather, the measured current often contains contributions from so-called parasitic processes:

$$I(U) = I_{\text{HER}}(U) + \sum_i I_{\text{parasitic},i} \quad (1)$$

Where the  $I_{\text{parasitic},i}$  denotes all charge transfer processes other than HER taking place. Typical examples include (i) the reduction of pre-oxidised catalyst/support or (ii) the reduction of catalyst/support material oxidized during cycling, as well as contributions from (iii) double-layer capacitance, (iv) electronic feedback from the potentiostat, (v) redox processes of products, (vi) under potential deposition (UPD) of species *e.g.* protons, (vii) reduction of the electrolyte *etc.*. By shifting from potentiodynamic to *quasi*-potentiostatic conditions some of these processes can be minimized by providing *quasi*-steady-state conditions. Nonetheless, determining the actual HER current is difficult with this kind of measurement. The Spectro Inlets' electrochemistry-mass spectrometry (EC-MS) enables quick and reliable detection of volatile electrochemical products such as H<sub>2</sub>. Thereby it allows the user to directly measure and quantify the evolved H<sub>2</sub>, eliminating the contribution from parasitic reactions and allowing them even to relate product signals with the faradaic charge transfer to obtain faradaic efficiencies.

In this application note, the use of the Spectro Inlets EC-MS for HER is demonstrated by simple HER experiments and by presenting HER related EC-MS literature.

## Examples of HER analysis using the EC-MS

Commercially available catalyst materials were investigated showcasing the EC-MS HER detection capabilities. This was done using four well-established catalysts, whereof Pt<sub>Poly</sub> was investigated in different electrolytes [5, 6]:

- Pt<sub>poly</sub> (PINE Inst., see [7] for proper preparation) in 0.1 M HClO<sub>4</sub>, 0.5 M H<sub>2</sub>SO<sub>4</sub> and under alkaline conditions in 0.5 M KOH.
- Pd/C NPs (TKK, 30 w%) on glassy carbon (GC) substrate in 0.1 M HClO<sub>4</sub>.
- Pt/C NPs (TKK, 46.7 w%) on GC substrate in 0.1 M HClO<sub>4</sub>.
- MoS<sub>2</sub> (non-PGM) nanoparticles (NPs) on GC substrate in 0.1 M HClO<sub>4</sub>.

HER investigations on Pt<sub>poly</sub> in three different electrolytes was chosen to highlight the differences in performance using a standard acidic electrolyte (H<sub>2</sub>SO<sub>4</sub>), a non-adsorbate-adsorbate interacting acidic electrolyte (HClO<sub>4</sub>), and an alkaline electrolyte (KOH). In alkaline conditions, lower HER activity of Pt is expected. Note, all potentials are given vs. the reversible hydrogen electrode (RHE) an extremely useful reference potential when conducting HER research.

### Experimental preparation

Prior to any measurements the EC-MS cell was cleaned in fresh "Piranha". For a description of the procedure see *Cleaning Procedures EC-MS Technical Note #12*. It is important to note that any trace amount of Pt (or Pd, Ir etc.) in the cell may contribute significantly in the HER response. Thus, before measuring non-PGM catalyst the cell and GC supports have to be thoroughly cleaned, ideally using *aqua regia* or fresh Piranha solution in combination with thorough rinsing with ultrapure water.

Catalyst systems relying on nanocatalysts were prepared by ink deposition on a GC support. Inks with Pt/C, Pd/C and MoS<sub>2</sub> were prepared using established protocols. Following this the cell was mounted with the GC stub and ink was dispensed using a pipette directly onto the GC substrate in the pre-assembled cell, see figure 2.

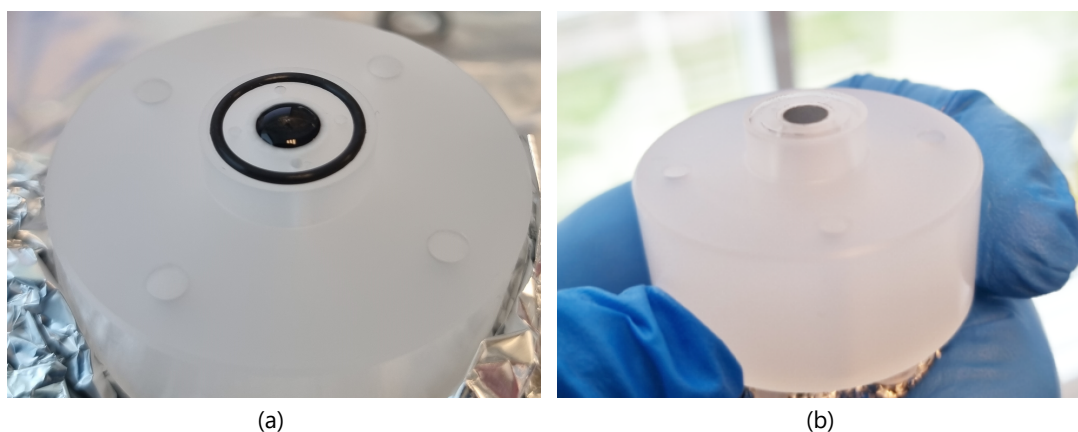


**Figure 2:** (a) Assembled cell with GC electrode whereupon 10 µL Pd/C ink has been deposited. (b) Same electrode after ink had dried in a uniform fashion.

Once the ink had dried, the cell was mounted onto the EC-MS using the standard procedure, for details see *EC-MS manual v1.15* and *Fluctuations due to Bubbles EC-MS Technical Note #11*. Importantly, the loading of the Pt/C and Pd/C electrodes differed significantly

from that of the MoS<sub>2</sub> sample, being *ca.* 25 μg/cm<sup>2</sup> and 1.1 mg/cm<sup>2</sup>, respectively. The reasons for the difference between PGM and non-PGM loading were three-fold:

- i) MoS<sub>2</sub> is a rather unstable HER catalyst, hence to get the appearance of a *quasi*-stable CV significant loading would be required (though not generally recommended as sensitivity to detecting stability issues decreases).
- ii) Having exceedingly high loading of a nano-porous catalyst layer should impose prolonged product retention, highlighting the EC-MS ability to visualize key transport limitations when conducting HER experiments.
- iii) A wide variation in loading emphasises that HER catalytic responses happen relative to the actual active catalyst area. Hence, two catalysts one with half the intrinsic activity but twice the total area may appear equally active, which is obviously not the case neither in terms of intrinsic/specific- nor mass activity.

Herein, we do not address issues related to mass loading or catalyst ECSA variation or how these parameters influence observed HER activities (more information concerning ECSA evaluation using the EC-MS system can be found in ***CO-stripping Technique EC-MS Application Note #1***).

## Experimental results

The six systems were tested following the procedure established in ***Benchmark Measurements EC-MS Technical Note #2***. Essentially, EC-MS responses were collected under potentiodynamic and *quasi*-potentiostatic conditions, specifically while conducting cyclic voltammetry (CV) and chronopotentiometry (CP). Representative experimental data can be seen in figure 3.

From figure 3 we note that when cycling to low potentials clearly detectable changes in *M2* signal from H<sub>2</sub> evolving at the electrode can be observed.

Instead of plotting raw mass signal vs. time one can co-plot a series of CVs (subsets of the raw data) vs. potential and use simple statistical tools with the Python package *ixdat*. This allows to calculate mean CVs and associated standard deviation. Doing such analysis highlights the potentiodynamic changes in H<sub>2</sub> signal when reaching sufficiently cathodic catalyst potentials as shown in figure 4 for all six HER catalyst systems.

Figure 4 highlights how the *M2* signal changes for all the catalysts systems when going sufficiently cathodic. It should be mentioned that Pd<sup>1</sup> and Pt-based catalyst are operated from *ca.* 0 to 1.05 V<sub>RHE</sub>, whereas MoS<sub>2</sub> is known to become excessively unstable above 0.2 V<sub>RHE</sub> in acidic conditions such as those employed [6], hence a potential range from -0.3 to 0.2 V<sub>RHE</sub> was chosen for this material.

The potentiodynamic current responses combined with the observed MS signal variations, as plotted in figure 4, highlight the EC-MS's ability to quickly provide the user with data on expected and/or unwanted gas evolution's onset potential(s), thus identifying potential ranges of interest. However, as described in the introduction, potentiodynamic measurements are prone to parasitic reactions.

<sup>1</sup>Work by *Mayrhofer et al.* [8] suggest Pd starts dissolving around 0.85 V<sub>RHE</sub> at pH 1.

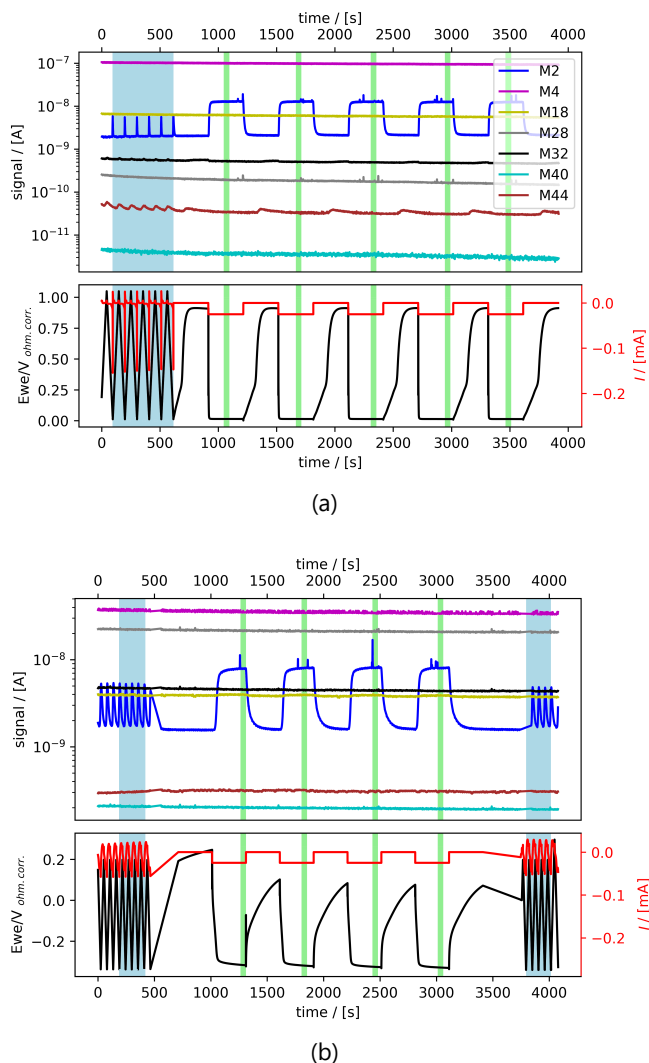


**Figure 3:** EC-MS experiments at room temperature in He-saturated electrolytes of (a) Pt<sub>Poly</sub> in 0.1 M HClO<sub>4</sub>. (b) MoS<sub>2</sub> in 0.1 M HClO<sub>4</sub>. Faded blue and green regions (seen as vertical bars) correspond to data ranges utilized for CV and CP analysis, respectively, as shown in the following. Masses correspond to *M2* = H<sub>2</sub>, *M4* = He, *M18* = H<sub>2</sub>O, *M28* = N<sub>2</sub>/CO, *M32* = O<sub>2</sub> and *M44* = CO<sub>2</sub>.

Using the experimental data presented in figures 4 and 5 as examples, in the following, we will discuss some of the most common effects of parasitic reactions occurring under different experimental conditions.

### Pt<sub>Poly</sub> in HClO<sub>4</sub>

A positive current peak is observed in the anodic scan in the HER region of figure 4a, indicating significant HOR, as the change in potential is imposed faster than the diffusion of H<sub>2</sub> away from the electrode. The integrated *M2* signal will therefore be lower than the amount if H<sub>2</sub> produced in the cathodic scan. However, over a series of six CVs, the relative

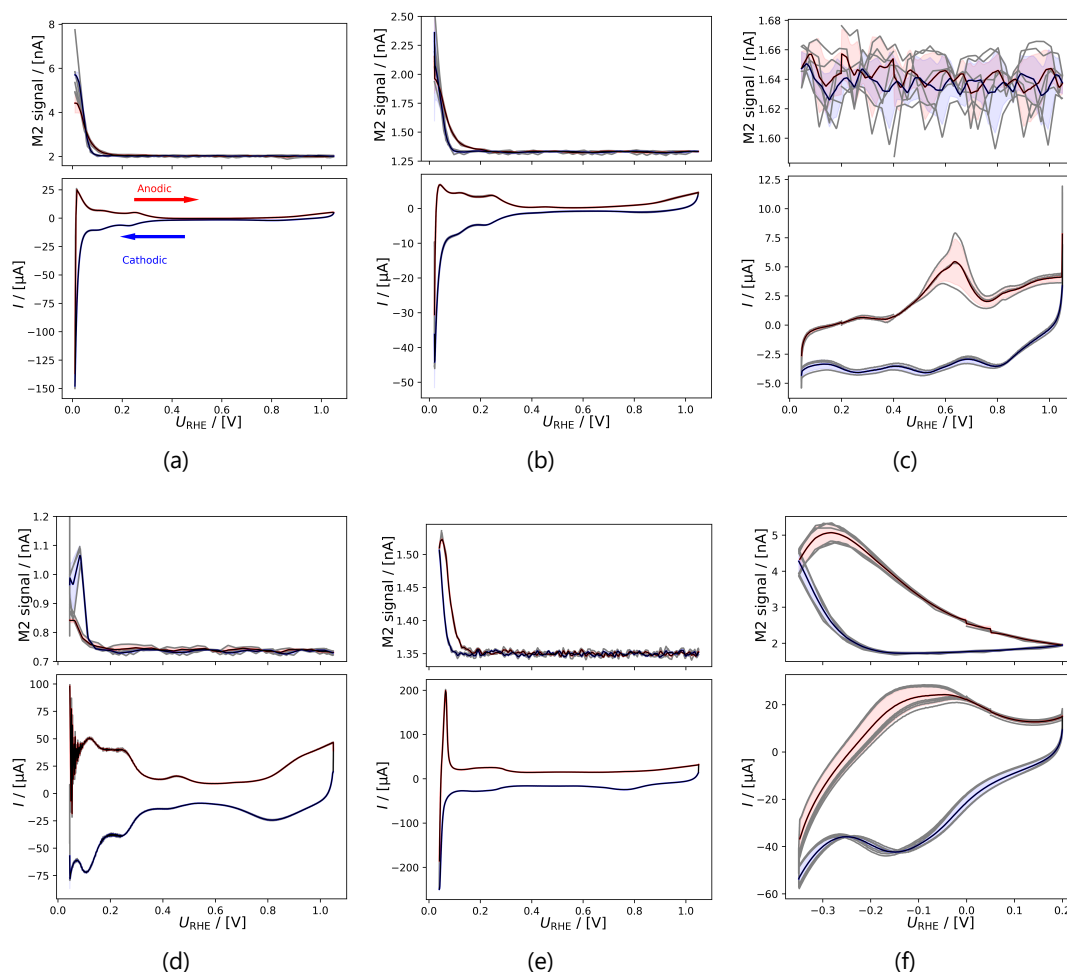


**Figure 4:** Averaged  $M2$  signals (top) and corresponding CVs (bottom), (a) of  $Pt_{poly}$  in 0.1 M  $HClO_4$ . (b) of  $Pt_{poly}$  in 0.5 M  $H_2SO_4$ . (c) of  $Pt_{poly}$  in 0.5 M  $KOH$ . (d) of Pt/C NPs in 0.1 M  $HClO_4$ . (e) of Pd/C NPs in 0.1 M  $HClO_4$ . (f) of  $MoS_2$  in 0.1 M  $HClO_4$ . All data was obtained at room-temperature at 20 mV/s in He-saturated electrolyte. Gray raw CV data, blue and red corresponds to averaged anodic and cathodic sweeps, respectively.

current vs.  $M2$  signal does not vary much as *i*) Pt is stable *ii*) and *pseudo* capacitances are insignificant relative to the HER current.

### $Pt_{poly}$ in $H_2SO_4$

The CVs of figure 4b appear to be offset below zero current, suggesting some  $O_2$  was available at the Pt electrode *i.e.* both HER and oxygen reduction reaction (ORR) took place.

### $Pt_{poly}$ in $KOH$

The HER onset potential in alkaline conditions is lower than in acid (*i.e.* the overpotential is higher). Hence, when using the same potential limits as shown in figure 4c, no  $H_2$  signal is observed in the MS: The  $M2$  signal is at baseline level. In the electrochemical current, a

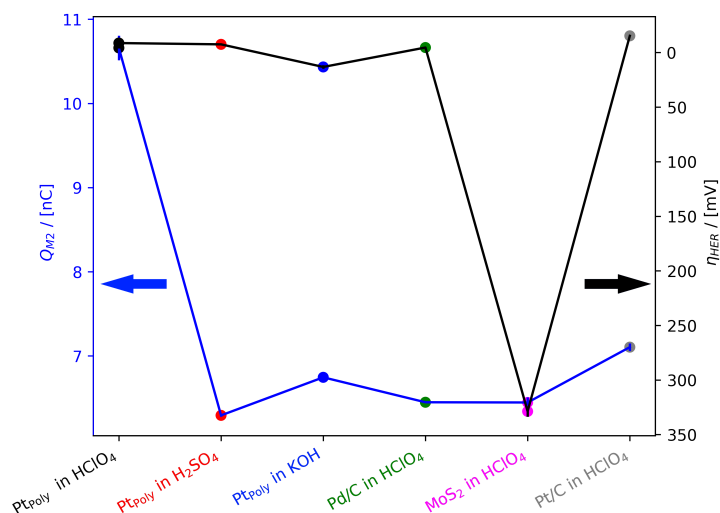


**Figure 5:** Overpotential  $\eta_{HER}$  derived from CP experiments @  $-0.25$  mA at room temperature co-plotted with corresponding integrated  $M2$  signals (integrated over 30 s under steady-state conditions).

peak is observed at ca.  $0.6$  V vs. RHE which varies significantly over the course of several cycles. It can be attributed to reactions of (bi)carbonates forming in aged KOH, making it impossible to accurately account for double-layer capacitance contributions to HER current.

#### Pt/C in HClO<sub>4</sub>

In figure 4d, the electrochemical current shows a typical sign of insufficient potentiostat feedback in the low potential region of the anodic scan. Such noise is common for potentiodynamic measurements, and can often be avoided by choosing the right potentiostat settings. If not completely eliminated, it will affect the accuracy of any integration of the current.

In contrast to the flat Pt<sub>poly</sub> sample, on Pt/C, a significant capacitance is observed, as well as the typical waves of hydrogen underpotential deposition (H-UPD) on Pt. From the current signals, the occurrence of HER is not evident, as it is largely obscured by H-UPD. Nonetheless, a clear  $M2$  signal is seen in the MS, highlighting the high sensitivity of the EC-MS enabling detection of HER onset prior to observation from the potentiostat!

#### Pd/C in HClO<sub>4</sub>

In figure 4e, again a HOR-related current is observed as a positive oxidative current after HER. Also here, this will negatively affect the accuracy of a charge transfer balance between  $M2$  and CV signals. Similarly to Pt/C, the *pseudo*-capacitance is significant due to the large area of the Pd/C catalyst. The charge transfer balance is additionally influenced as Pd is known to form hydrides below  $0.2 V_{RHE}$  [9] This is of minor importance on nanoparticles as used here, where the surface is large compared to the bulk, however it will have a more significant contribution to the electrochemical current if some form of bulk metal is used.

## MoS<sub>2</sub> in HClO<sub>4</sub>

While significantly active for HER, MoS<sub>2</sub> requires a rather high catalyst loading compared with noble metal catalysts, which has following effects seen in figure 4f: *i)* The *pseudo* capacitance is even more significant than observed for Pt/C and Pd/C, obscuring even further the HER contribution to the CV charges. *ii)* Poor transport of produced hydrogen through the porous and thick catalyst layer, which imposes a prolonged *M2* signal response. *iii)* The number of ill defined/multiple active sites on this catalyst imposes continuous oxidation and reduction events, exacerbated by the significant loading. Also such effects can be considered parasitic processes and need to be considered in data analysis and interpretation.

## General observations

As evident from the discussion above, parasitic reactions play a significant role on most HER catalyst materials, but are often difficult to distinguish from HER current. The EC-MS allows to measure H<sub>2</sub> completely separately from the electrochemical processes. Calibration of the *M2* signal following recommendations presented in ***EC-MS Quantification - EC-MS Application Note #2*** allows for full quantification of HER activity from the MS data, eliminating the need for cumbersome identification and removal of parasitic current contributions from the electrochemical data.

Note, however, that the sensitivity of the instrument will change over time when using the electron multiplier detector, resulting in different *M2* signals measured for the same amount of H<sub>2</sub> produced. An example for this can be seen in figure 5: At the same current density, the *M2* charge on Pt<sub>Poly</sub> in 0.1 M HClO<sub>4</sub> appears to be higher than in other electrolytes or on other sample. This could be interpreted as an indication that there are significant parasitic processes happening in all other systems, even during steady-state conditions. However, looking more closely in figure 3, it is evident that not only *M2*, but also *M4*, the mass fragment from the make-up gas He, is lower in intensity. This indicates, that the sensitivity of the mass spectrum had decreased significantly in the meantime, resulting in this drop in *M2* intensity. Changes in MS sensitivity need to be considered appropriately, as discussed in detail in ***EC-MS Quantification - EC-MS Application Note #2***.

Note, that when estimating the actual HER/HOR activity of a catalyst, the electrolyte should be saturated with H<sub>2</sub> throughout the experiment (i.e. via H<sub>2</sub> make-up gas).

## HER relevant studies using the EC-MS in literature

Significant insight into HER can be acquired using the Spectro Inlets EC-MS system - insight relevant both for the commercial development of HER technologies (electrolyzers, nano-material producers *etc.*) as well as the scientific electrocatalytic community as a whole. HER studies often incorporate reference measurements to Pt. Work by *Trimarco et al.* [10] highlights typical Pt performance and shows a CO-stripping experiment (also see ***CO-stripping Technique EC-MS Application Note #1***), to determine the catalyst surface area. In the following, we provide examples of the unique insights generated by the EC-MS along with highlighted publications demonstrating specific use cases. We suggest researchers

commencing similar research projects to acquaint themselves with relevant EC-MS literature.

## Identification of parasitic HER current and faradaic efficiencies

While a target reaction in water electrolysis, HER is considered a parasitic reaction for other electrochemical reduction reactions *e.g.* the CO<sub>2</sub> reduction reaction (eCO<sub>2</sub>RR), CO reduction reaction (eCORR) as well as nitrogen and nitrate/nitrite reduction eN<sub>2</sub>RR and eNO<sub>x</sub>RR. For examples of the EC-MS's ability to accurately evaluate electrocatalytic reduction reactions we refer to the work by *Hochfilzer et al.* [11, 12] concerning eCORR, work by *Krzydwa et al.* [13, 14] concerning eNO<sub>x</sub>RR and work by *Krempl et al.* [15]. A great strength of the EC-MS, in relation to reduction electrochemistry comes from its inherent ability to provide the user with quantifiable measures of volatiles produced at the electrode interface. Thereby enabling evaluation of faradaic efficiencies, turn-over-frequencies and product selectivity for gaseous and volatile liquid products.

A different aspect of parasitic HER concerns catalyst support materials. A rigorous statistical analysis using the EC-MS was conducted by *Oates et al.* [16] recently, which revealed that HER activity in carbon is mainly facilitated by residual metal content operating as active sites. This was established not by the potentiostat data but from careful EC-MS H<sub>2</sub> calibration enabling to completely exclude contributions from other charge transfer processes, such as graphene oxide reduction *etc.*, from the HER activity analysis.

## Modelling HER and H<sub>2</sub> transport

Work by *Krempl et al.* [17] establishes a basic model for the mass transport properties of H<sub>2</sub> in the EC-MS. Using such a model can, for example, be beneficial for resolving transient processes of duration even shorter than the <1 s time response of the EC-MS. Such studies may also help gauge H<sub>2</sub> transport for a wide variety of HER applications.

## Hydride studies

Several EC-MS studies investigate the electrochemical properties of Cu, an important catalyst for eCO<sub>2</sub>RR. During cathodic potentials, Cu performs differently in various electrolytes. These changes are most often observable in the Cu electrodes' CVs at or close to HER conditions.

Works by *Scott et al.* [18] and *Tacket et al.* [19] have been instrumental in revealing that Cu, under certain conditions, forms Cu hydrides (Cu-H). These Cu-H's are stable up to above 0V<sub>RHE</sub>, meaning H<sub>2</sub> signal can be observed above the RHE potential. *Tacket et al.* combined the EC-MS observations with *Raman* spectroscopy thereby proving the Cu-H formation on Cu(111) single-crystals. This demonstrates clearly the usefulness of the EC-MS system both as a standalone piece of laboratory equipment, but also the EC-MS's ability to provide additional insights when combined with other laboratory techniques.

Besides the aforementioned, the EC-MS enables wide range of electrochemical studies. Especially, when combined with careful calibration. For such quantification purposes of H<sub>2</sub> we refer to *EC-MS Quantification - EC-MS Application Note #2*.

## Summary

In this application note, we demonstrated the advantages of using a Spectro Inlets EC-MS for studying different HER catalyst materials. We highlighted how measuring the produced H<sub>2</sub> can eliminate inaccuracies often introduced when using the electrochemical current as a proxy for the HER reaction rate.

## References

- [1] S. Chu, Y. Cui, and N. Liu, "The path towards sustainable energy," *Nature Materials*, vol. 16, no. 1, pp. 16–22, 2016. DOI: [10.1038/nmat4834](https://doi.org/10.1038/nmat4834).
- [2] I. T. McCrum and M. T. Koper, "The role of adsorbed hydroxide in hydrogen evolution reaction kinetics on modified platinum," *Nature Energy*, vol. 5, no. 11, pp. 891–899, 2020. DOI: [10.1038/s41560-020-00710-8](https://doi.org/10.1038/s41560-020-00710-8).
- [3] C. C. McCrory, S. Jung, I. M. Ferrer, S. M. Chatman, J. C. Peters, and T. F. Jaramillo, "Benchmarking hydrogen evolving reaction and oxygen evolving reaction electrocatalysts for solar water splitting devices," *Journal of the American Chemical Society*, vol. 137, no. 13, pp. 4347–4357, 2015. DOI: [10.1021/ja510442p](https://doi.org/10.1021/ja510442p).
- [4] C. Roy *et al.*, "Impact of nanoparticle size and lattice oxygen on water oxidation on nifeoxy," *Nature Catalysis*, vol. 1, no. 11, pp. 820–829, 2018. DOI: [0.1038/s41929-018-0162-x](https://doi.org/10.1038/s41929-018-0162-x).
- [5] R. Makharia *et al.*, "Durable pem fuel cell electrode materials: Requirements and benchmarking methodologies," *ECS Transactions*, vol. 1, no. 8, pp. 3–18, 2006. DOI: [10.1149/1.2214540](https://doi.org/10.1149/1.2214540).
- [6] J. Kibsgaard and T. F. Jaramillo, "Molybdenum phosphosulfide: An active, acid-stable, earth-abundant catalyst for the hydrogen evolution reaction," *Angewandte Chemie - International Edition*, vol. 53, no. 52, pp. 14 433–14 437, 2014. DOI: [10.1002/anie.201408222](https://doi.org/10.1002/anie.201408222).
- [7] J. Clavilier, R. Faure, G. Guinet, and R. Durand, "Preparation of monocrystalline pt microelectrodes and electrochemical study of the plane surfaces cut in the direction of the 111 and 110 planes," *Journal of Electroanalytical Chemistry and Interfacial Electrochemistry*, vol. 107, no. 1, pp. 205–209, 1980, ISSN: 0022-0728. DOI: [https://doi.org/10.1016/S0022-0728\(79\)80022-4](https://doi.org/10.1016/S0022-0728(79)80022-4).
- [8] E. Pizzutilo *et al.*, "Palladium electrodisolution from model surfaces and nanoparticles," *Electrochimica Acta*, vol. 229, pp. 467–477, 2017. DOI: [10.1016/j.electacta.2017.01.127](https://doi.org/10.1016/j.electacta.2017.01.127).
- [9] A. Rose, S. Maniguet, R. J. Mathew, C. Slater, J. Yao, and A. E. Russell, "Hydride phase formation in carbon supported palladium nanoparticle electrodes investigated using in situ exafs and xrd," *Phys. Chem. Chem. Phys.*, vol. 5, pp. 3220–3225, 15 2003. DOI: [10.1039/B302956E](https://doi.org/10.1039/B302956E).

- [10] D. B. Trimarco *et al.*, "Enabling real-time detection of electrochemical desorption phenomena with sub-monolayer sensitivity," *Electrochimica Acta*, vol. 268, pp. 520–530, 2018, ISSN: 0013-4686. DOI: <https://doi.org/10.1016/j.electacta.2018.02.060>.
- [11] D. Hochfilzer *et al.*, "Transients in electrochemical CO reduction explained by mass transport of buffers," *ACS Catalysis*, vol. 12, no. 9, pp. 5155–5161, 2022. DOI: [10.1021/acscatal.2c00412](https://doi.org/10.1021/acscatal.2c00412). eprint: <https://doi.org/10.1021/acscatal.2c00412>.
- [12] D. Hochfilzer, J. E. Sørensen, E. L. Clark, S. B. Scott, I. Chorkendorff, and J. Kibsgaard, "The importance of potential control for accurate studies of electrochemical CO reduction," *ACS Energy Letters*, vol. 6, no. 5, pp. 1879–1885, 2021. DOI: [10.1021/acsenenergylett.1c00496](https://doi.org/10.1021/acsenenergylett.1c00496). eprint: <https://doi.org/10.1021/acsenenergylett.1c00496>.
- [13] P. M. Krzywda, A. Paradelo Rodríguez, N. E. Benes, B. T. Mei, and G. Mul, "Effect of electrolyte and electrode configuration on Cu-catalyzed nitric oxide reduction to ammonia," *ChemElectroChem*, vol. 9, no. 5, e202101273, 2022. DOI: <https://doi.org/10.1002/celec.202101273>. eprint: <https://chemistry-europe.onlinelibrary.wiley.com/doi/pdf/10.1002/celec.202101273>.
- [14] P. M. Krzywda, A. Paradelo Rodríguez, L. Cino, N. E. Benes, B. T. Mei, and G. Mul, "Electroreduction of NO<sub>3</sub><sup>-</sup> on tubular porous Ti electrodes," *Catal. Sci. Technol.*, vol. 12, pp. 3281–3288, 10 2022. DOI: [10.1039/D2CY00289B](https://doi.org/10.1039/D2CY00289B).
- [15] K. Krempel *et al.*, "Quantitative operando detection of electro synthesized ammonia using mass spectrometry," *ChemElectroChem*, vol. 9, no. 6, e202101713, 2022. DOI: <https://doi.org/10.1002/celec.202101713>. eprint: <https://chemistry-europe.onlinelibrary.wiley.com/doi/pdf/10.1002/celec.202101713>.
- [16] R. P. Oates *et al.*, "How to minimise hydrogen evolution on carbon based materials?" *Journal of The Electrochemical Society*, vol. 169, no. 5, p. 054 516, May 2022. DOI: [10.1149/1945-7111/ac67f7](https://doi.org/10.1149/1945-7111/ac67f7).
- [17] K. Krempel *et al.*, "Dynamic interfacial reaction rates from electrochemistry–mass spectrometry," *Analytical Chemistry*, vol. 93, no. 18, pp. 7022–7028, 2021, PMID: 33905662. DOI: [10.1021/acs.analchem.1c00110](https://doi.org/10.1021/acs.analchem.1c00110). eprint: <https://doi.org/10.1021/acs.analchem.1c00110>.
- [18] S. B. Scott *et al.*, "Anodic molecular hydrogen formation on Ru and Cu electrodes," *Catal. Sci. Technol.*, vol. 10, pp. 6870–6878, 20 2020. DOI: [10.1039/D0CY01213K](https://doi.org/10.1039/D0CY01213K).
- [19] B. M. Tackett, D. Raciti, A. R. Hight Walker, and T. P. Moffat, "Surface hydride formation on Cu(111) and its decomposition to form H<sub>2</sub> in acid electrolytes," *Journal of Physical Chemistry Letters*, vol. 12, no. 44, pp. 10 936–10 941, 2021. DOI: [10.1021/acs.jpcllett.1c03131](https://doi.org/10.1021/acs.jpcllett.1c03131).

All data treatment and plotting in this application note was carried out using the open source Python package *ixdat*, available at <https://github.com/ixdat/ixdat>.